ENHANCED HYDRODYNAMICS OF PLANING HULL USING ENERGY SAVING DEVICES

S Jangam, AMET University, Chennai, India,

ABSTRACT

In calm water conditions, the moving planing vessels in semi-planing mode release the majority of their energy from the hull to the water. Depending on the Froude number, these moving vessels produce a Kelvin wave pattern in calm water. The Volume of Fluid (VOF) approach uses the overset grid method in a RANSE-based CFD solver to track the interface between water and air. The resistance components of a planing hull were computed using the obtained results. Data from experiments are compared with the numerically simulated findings. It is seen that the resistance values predicted by the numerical simulation results are in close agreement with the experimental results for the hull equipped with the interceptor. This work aims to record the wave profile, resistance, and trim at the free surface at the transom for different beam Froude numbers. The findings are compiled for hull placed on a high-speed planing ship with a 20 degree deadrise angle, both with and without an integrated interceptor-flap. For the hull with integrated interceptor-flap, there is a reduction in drag of 19-24%, trim of 50-53%, and the free surface wave elevation of 25-40% at the transom, which contributes to the vessel's overall performance improvement.

Key words: Planing hull, interceptor, flap, resistance, trim, free surface wave.

NOMENCLATURE

B	Breadth of vessel	S	Span of flap
CFD	Computational Fluid Dynamics	V	Speed of hull
C	Chord of flap	VOF	Volume of Fluid
Fn_B	Beam Froude number	ν	Kinematic viscosity of fluid
f_{bi}	Body force	μ	Dynamic viscosity coefficient
ITTC	International Towing Tank Conference	Δt	Time-step
L_k	Wetted Keel length	g	Acceleration due to gravity

1. INTRODUCTION

In calm waters, the energy of a moving ship is released as waves. Ship hydrodynamics includes the study of the generated wave pattern as one of its fundamental subjects. When the ship is moving, the waves it creates can disperse a significant distance from their source. The friction across the hull's wetted surface creates a net force that opposes the ship's motion when it is going through the water. The wetted hull surface, surface roughness, and water viscosity all affect this frictional resistance. Therefore, a lot of work goes into modelling and researching the flow pattern around the ship using potential and turbulent flow methods. Numerical potential algorithms were employed by Jensen et al. [15] and Larsson et al. [17] to solve wave resistance issues. But for high Reynolds numbers, the turbulent flow models are used.

The governing Reynolds Averaging Navier-Stokes (RANS) equations are solved numerically using finite volume method (FVM).

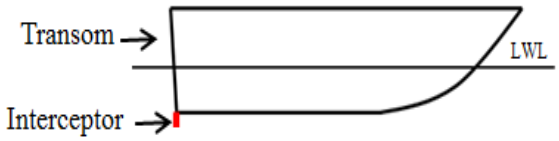

a. With interceptor

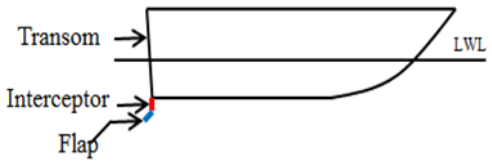

b. With interceptor-flap

Figure 1: Schematic diagram of stern interceptor and interceptor-flap

To capture the wave profile on the free surface surrounding the hull, researchers have been utilising simulation models that need a lot of processing power. By utilising the perturbation approach to incorporate a free surface boundary condition, Dawson [7] discovered wave resistance and predicted the Kelvin wave. Additionally, in order to assess the free surface and examine the surrounding flow on the yacht, Xia [33] combined Dawson [7].

Tuck et al. [30] created a computational code to investigate wave patterns. Using linearized water wave theory, their work on wave resistance for high-speed vessels provided precise information of the wave pattern and pressure distribution in both near and far fields. Kim et al.'s [14] numerical investigation of turbulent free-surface flow was carried out on a self-propelled KRISO 138K utilising a finite volume based RANS model.

Sadathosseini et al. [23] do numerical studies on a circular cylinder and surface-piercing bodies of NACA0024 foil for various Froude numbers. It offered insight into the wave-induced free surface separation issue. Ansys CFX simulations on a DTMB 5415 model with two distinct internal grid structures utilised numerical flow prediction over the free surface at two distinct Froude values (Ahmed et al., [3]). Their research showed that it is possible to achieve better outcomes by reducing the number of computational grid elements by employing hybrid mesh. Javanmardi et al., [16] conducted experimental and numerical studies to estimate the wave pattern surrounding the hull in limited waterways. The investigation came to the conclusion that wave heights could be captured using the FLUENT CFD programme. A numerical investigation on hydrofoils using NACA 0012 and Wigley hulls was carried out by Adjali et al. [2]. The free surface water wave was captured using the VOF approach with less computational grid elements, yielding good results.

Transom appendages such as flaps, trim tabs, and stern wedges have been used recently to evaluate the hydrodynamic performance of high-speed planing hulls, destroyers, and semi-displacement hulls (Seo et al., [25]). The interceptor, a stern extension, is evolved from transom flaps. The interceptor is a longer plate that descends vertically while maintaining the transom's form. Figure 1a depicts the schematic diagram of the interceptor plate installed close to the planing hull's transom, while Figure 1b shows the interceptor and flap together. Hydrodynamic parameter capture in experiments is costly and difficult. In order to forecast the hull's running trim, drag, and free surface pattern, very intensive computer models come in help.

However, for the hull with interceptor and flap combination, the fluid flow properties and free surface wave pattern are not recorded experimentally. Brizzolara [4] conducted a simplified 2D research on the interceptor by utilising the RANSE code to analyse the pressure and velocity distributions at the transom. Villa and Brizzolara conducted a comparison of the effects of flaps and interceptors on hull performance [32]. Ghassemi et al.'s numerical investigations on the hydrodynamic forces of a planing hull with an interceptor [9] revealed decreased trim by the vessel's aft. Numerical studies on displacement hulls and semi-planing hulls with spray rails equipped with interceptors and stern flaps were carried out by Salas et al. [24]. They observed that the semi-planing hull experiences a greater reduction in resistance. Mansoori et al. [19] conduct both computational and experimental studies to examine the impact of an interceptor and deadrise angle on a planing hull. Suneela et al. [26] investigated the performance of a planing hull equipped with a combing interceptor-flap using the single grid option in the RANSE solver. Song et al.'s [27] numerical research on a waterjet-powered ship equipped with an interceptor revealed that the upstream flow close to the interceptor is what drives variations in the entrance velocity distribution.

Studies on free surface flow for hydrofoils, semi-displacement hulls, and various displacements were conducted. The majority of research on planing hulls discovered the impact of trim and resistance when installing interceptors or flaps separately. In order to better understand the fluid flow behaviour at the transom near the interceptor, the free surface is recorded. This information helps designers improve the performance of boats equipped with interceptors that will soon have a 20-degree deadrise. Furthermore, there is a dearth of research on free surface flow, and the hull with interceptor and flap combination at transom for planing hulls has been the subject of extremely little literature.

Several researchers have recently become interested in analysing the hydrodynamics of the combing interceptor-flap at varying speeds. This study tries to improve the planing vessel's performance both with and without an interceptor, as well as with an interceptor-flap combination and a 20 degree deadrise angle. This study makes use of the commercial RANS-based CFD solver STAR CCM+. In addition, a computational model is developed and simulations are run for the hull at various speeds, both with and without an interceptor and interceptor-flap. The planing hull with and without an interceptor was tested in the towing tank at the Indian Institute of Technology Madras' Department of Ocean Engineering. The computational solver's accuracy was confirmed by the outcomes of the experiments. The work is continued to replicate free surface wave height in calm water at different speeds for the hull with and without interceptor and integrated interceptor-flap. Initially, the resistance and running trim of the vessel are calculated numerically. Computational display aids in the reproduction of the basic fluid flow. Section 2 presents the approach utilised in the CFD programme to carry out the numerical calculations. Verification and validation results are covered in Section 3; results and comparisons are covered in Section 4; a summary and conclusions are then presented.

2. NUMERICAL SIMULATION METHODOLOGY

In order to examine the flow characteristics, numerical modelling can be utilised to duplicate the solution accurately and at a constant speed. For the flow simulation in this investigation, a commercial RANSE-based CFD code is utilised. The simulations for the hull with and without interceptor and integrated interceptor-flap fitted near the transom of planing hull are carried out using CFD code. Further, the dynamic changes in trim and drag of the hull for different Froude numbers are also noted. The kinematic aspect of free surface wave flow of the hull is also simulated, besides estimating drag and running trim.

2.1 GOVERNING EQUATIONS

The vessel's dynamic changes are simulated by numerical modelling. Experimental data is used to validate and compare the numerical results. The fluid flow phenomena is governed by continuity and momentum equations. The viscous flow of fluid is assumed to be incompressible in ship hydrodynamics. Hence, the differential form of the Navier Stokes equations combined with Reynolds averaged form of the N-S equation (RANSE) are used. For viscous fluid, RANS equations are globally compatible control equations of kinematics. The incompressible viscous flow field around the floating body is simulated with RANS equation.

The RANS equation is defined as

$$\frac{\partial \rho}{\partial t} + \frac{\partial (\rho u_i)}{\partial x_i} = 0 \qquad (1)$$

The formulation for momentum is written as

$$\frac{\partial (\rho u_i)}{\partial t} + \frac{\partial (\rho \overline{u_i u_j})}{\partial x_j} = -\frac{\partial p}{\partial x_i} + \frac{\partial}{\partial x_j}[\mu \frac{\partial u_i}{\partial x_j} + \frac{\partial u_i}{\partial x_i} - \frac{2}{3}\delta_{ij}\frac{\partial u_i}{\partial x_i}] + \frac{\partial}{\partial x_j}(-\rho \overline{u_i' u_j'}) + f_{bi} \qquad (2)$$

where,

p - Static pressure

ρ- Fluid density

μ - Dynamic Viscosity coefficient

' - Fluctuation component in the Reynolds Averaging

f_{bi} - Body force

δ_{ij} - Kronecker Delta

VOF method is used to stimulate the two-phase flow and also to capture the free-surface between water and air. In the VOF method, a function c is defined where the value of c is between zero and one when free surface exists. The solution equation is given as

$$\frac{\partial c}{\partial t} + \nabla.(uc) = 0 \qquad (3)$$

Hence the free surface is determined and is tracked. The transported variables in the k-ε turbulence model are k and ε, where k is the turbulence kinetic energy and ε is the rate of dissipation of turbulence energy (Prasad et al., [20]). The VOF formulation depends on the water and air near free surface which are not interpenetrating. For each additional phase in the computational cell a variable is introduced with volume fraction of phase. The sum of volume fractions of all phases should be equal to unity in each control volume. The water-air interface which is free surface, is properly modelled to simulate the flow around the vessel.

2.2 NUMERICAL SET-UP

In order to capture the flow phenomenon, a rectangular domain is computationally produced in the numerical modelling. The domain's borders are spaced enough apart from the hull to prevent fluid flow reflection (Fig 2). The coordinate system is fixed in such a way that the x-axis overlaps with the free surface and pointed downstream in calm water whereas the z-axis is pointed in the opposite direction to the acceleration due to gravity. The direction of free-stream velocity is in the direction of positive x-axis, denoted by U.

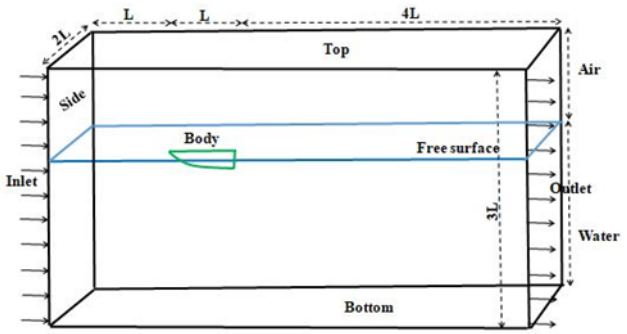

Figure 2: Schematic diagram of computational domain with boundary conditions.

Computational domain extends one length of vessel, L from the stem which is inlet boundary, 4L behind the stern of the ship as outlet boundary, 2L below the keel as bottom boundary and L to the side of the ship as wall boundary, where L represents the length of the ship. The dimensions considered for the computational domain are consistent with the ITTC 7.5-03-02-03[13] recommendations. There are no defined recommendations for the overset region in terms of domain dimensions (Tezdogan et al. [31]). It is assumed that the flow around the hull is symmetrical with respect to the centre plane. This assumption of symmetry promotes primary cut back of computational time. The boundary condition used in CFD is in accordance with ITTC guidelines [13].

Table 1: Parameters of the planing hull

Input data	**Symbols**	**Value**	**Unit**
Length	L	20	m
Breadth	B	5.3	m
Displacement	Δ	46000	kg
LCG from transom		6.5	m
Interceptor height	h	25	mm
Flap chord	C	2.5%L	m
Flap span	S	2.65	m
Design speed	V	25	knots
Acceleration due to gravity	g	9.81	m/s^2
Beam Froude number	Fn	1.78	No unit
Density of sea water	ρ	1025	kg/m^3
Reynolds number	Re	179323.6	No unit

Scale 1:25

The planing hull model used for numerical study is shown in Fig 3 mounted with integrated interceptor-flap at the transom where S is span of the flap and C is chord of the flap. RANSE based CFD solver is used for performing the simulations. Besides resistance and trim of the vessel, the free surface elevation of hull with interceptor-flap combing is captured.

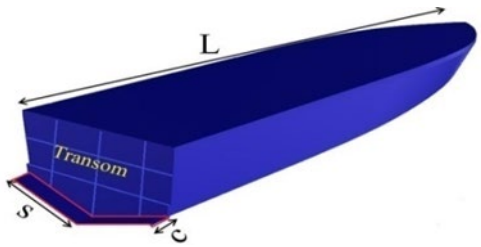

The flow related to ship is mostly large Reynolds number and is hence turbulent. Therefore, Navier Stokes equations are applicable for laminar as well as turbulent flows which express mass and momentum conservation of the flow.

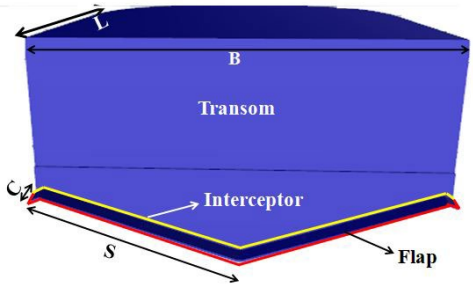

Model dimensions of flap:
L= Length of vessel =0.82m
B=Vessel beam =0.212m
S=Span of flap=106mm
C=Chord of flap=21.75mm

Figure 3: CAD model of the hull with interceptor and flap combination

The realisable k-ε turbulence model is used to capture the flow near free surface. This turbulence model also obtains the mean flow characteristics for turbulent flow conditions. Table 2 shows the solver parameters used in the simulation. VOF method which is simple multiphase model, is used to simulate the flow on numerical grids capable of resolving the interface between air and water. The interface between background mesh and overset mesh is created by linear interpolation scheme (De Luca et al., [8]). The interpolation function builds the coefficient matrix of algebraic equation system and simultaneously determines active cells in all regions (CD-Adapco [6]).

The generation of mesh has direct impact on the reliability of results. Overset grid option is used in the study which has background mesh and overset mesh (Fig 4). The background mesh is static, whereas the overset mesh is dynamic which moves along with the vessel. The function of speed of vessel (V) and keel wetted length (L_K) are used as the time-step in simulations, which are evaluated from Equation 4, according to ITTC [13].

$$\Delta t = 0.005 * \frac{L_K}{V} \qquad (4)$$

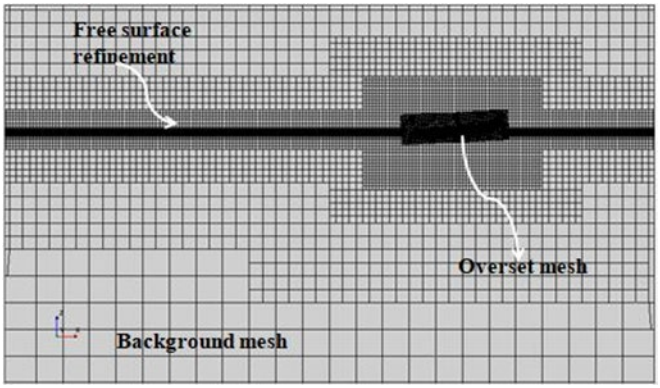

Figure 4: Background and overset mesh

The boundary layer flow is captured by generating the prism layers adjacent to the hull surface. Prism cells are generated on the hull surface to resolve the boundary layer. The wind and current speed are in opposite direction to ship velocity. The wall y+ value which is recommended range on wall function application for the high y+ wall treatment model is kept between the range of 30 and 130 over the hull (CD-Adapco [6]). All the simulations are performed until steady state is reached. The resistance and trim reaches the steady state when the solution is converged and the residual of all variables becomes constant.

Table 2: Solver parameters

Parameter	Settings
Solver	3D, Unsteady, Implicit
Turbulence model	Realizable k-ε
Pressure-velocity coupling	SIMPLE
Multiphase model	The volume of Fluid(VOF)
Wall treatment	Two layers all wall y+ treatment
Time discretization	First order upwind
Number of inner iterations	10
Overset interpolation scheme	Linear

2.3 GRID INDEPENDENT STUDY

The coarser, medium and fine grid was generated to carry out the grid independent study. This study was carried out for Fn=1.78 in calm water as shown in Table 3. Grid independent study is carried out to obtain reliable values. Based on grid refinement ratio of √2, the minimum cell size near the hull surface is multiplied by √2 to get the next grid. Grid B is selected from the grid independent study for the numerical simulation process.

Table 3: Grid independency study at Fn=1.78

Grid.	Cell count (million)	R_t/disp. (N/kg)	Trim (deg)
A	1.34	1.45	6.54
B	1.92	1.51	6.68
C	2.81	1.53	6.82
Experiment	-	1.49	6.65

3. VALIDATION OF NUMERICAL SIMULATION METHOD

The validation of numerical study is done with the experimental results as shown in Fig 1 for the bare hull. Parameters with their values used in the validation study are shown in Table 1. Resistance and trim for different speeds of the bare hull model is shown in Fig 5. The beam Froude number is given by $Fn_B = V/\sqrt{gB}$, where V is the speed of the hull, g is the gravitational acceleration and B denotes breadth of the vessel. Both numerical and experimental studies follow the same trend. The CFD results when compared with experimental results, it showed the resistance of the bare hull is in better correspondence with CFD results, and are used for validation purposes.

Model resistance tests were carried out at the Department of Ocean Engineering, IIT Madras towing tank, India. The hull model was geometrically similar, and scale ratio of the model is 1:25. The scaled model was considered based on the highest stable speed available with towing carriage facility.

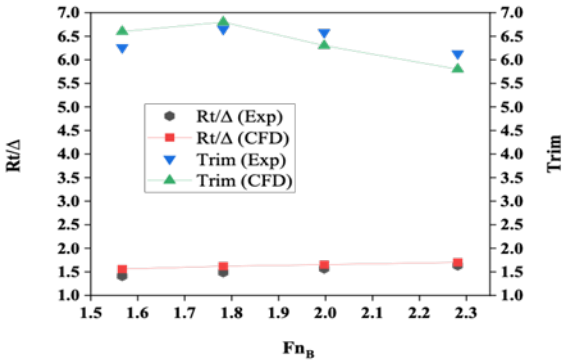

Figure 5: Experimental and CFD results for bare hull at different beam Froude numbers

The hull model was attached to the support frame of towing carriage, and the model was free to sink and trim. Model tests were carried out in a speed range of 1.0<Fn<2.28. Model test and wave patterns at Fn = 1.78 for bare hull are shown in Fig 6 and 7.

Figure 6: Wave pattern of bare hull model (exp) at Fn=1.78

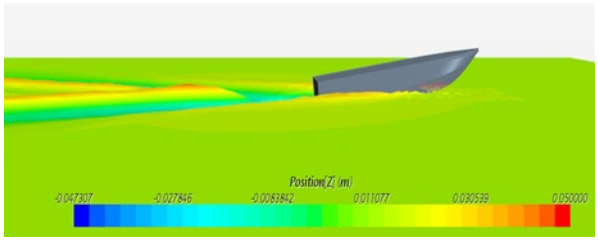

Figure 7: Wave pattern of bare hull model (numerical simulation) at Fn=1.78

The bare hull resistance was calculated numerically for Fn=1.57, 1.78, 2.0 and 2.28. Table 4 shows the computational resistance compared with experimental result for bare hull at different Froude numbers. Table 5 shows the computational resistance compared with experimental result for bare hull at different Froude numbers respectively.

Table 4: Computational resistance compared with experimental result for bare hull at different Froude numbers

Fn	R_t (Experimental)	R_t (Numerical)
1.57	4.15	4.58
1.78	4.38	4.76
2.0	4.61	4.86
2.28	4.81	5.02

Table 5: Computational trim compared with experimental result for bare hull at different Froude numbers

Fn	Trim (Experimental)	Trim (Numerical)
1.57	6.26	6.6
1.78	6.65	6.8
2.0	6.58	6.3
2.28	6.13	5.8

4. RESULTS AND COMPARISON

The overset grid option is utilised because it produces better related results for moving bodies,. This study compares the trim and resistance for interceptor, interceptor-flap, and bare hull. The free surface wave pattern and wave elevation with interceptor and interceptor-flap are also presented for different Froude numbers in this section.

4.1 RESISTANCE AND TRIM

An integrated interceptor-flap with different flap with different angular orientations of 0, 4, 8 deg was numerically simulated. Interceptor and flap with 4 deg showed good resistance reduction and trim angle on the vessel in comparison with other flap angles. The interceptor and flap combination is compared with and without interceptor also.

Table 6: Resistance and trim with interceptor for different flap angular orientations at Fn=1.78

Appendage	R_t/Δ (N/kg)	Trim (deg)
Interceptor-0 deg flap	1.41	4.7
Interceptor-4 deg flap	1.22	2.9
Interceptor-8 deg flap	1.20	1.7

Table 6 shows the resistance and trim for the hull fitted with interceptor and different angular orientations at Fn=1.78. Different flap angle configurations performed well with reduction in resistance and trim. When interceptor-4deg flap is considered it has better performance in comparison with 0 and 8 deg flap angles at Fn=1.78. Moreover, in planing hulls, the resistance increases with increase in speed. Interceptor-0deg shows reduction in resistance and trim when compared with bare hull. Interceptor-8deg also shows reduction in resistance and trim but tends to trim by bow with more pressure created at stern. However, interceptor-4deg shows better performance compared to other flap angle configuration with interceptor.

The benefits achieved using interceptor-4deg flap combination is that there is further reduction in resistance, trim and wave elevation at the stern due to which the performance of vessel is improved. Therefore, this combination of interceptor-flap seems to give better performance than those of individual appendages.

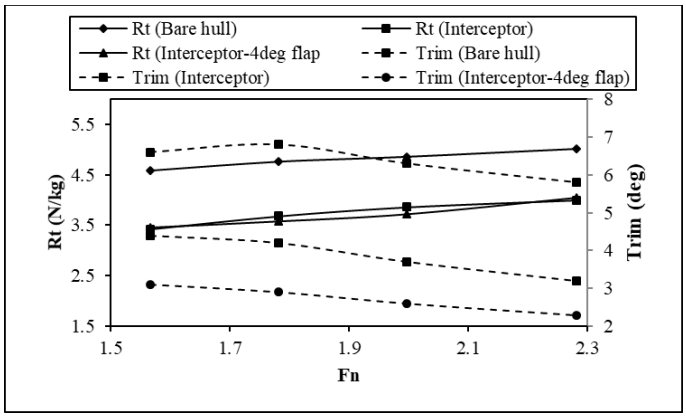

Figure 8: Comparison of resistance and trim for barehull and with interceptor and interceptor-4deg flap at different beam Froude numbers.

The resistance and trim of interceptor-flap 4 deg is less compared to the hull with and without interceptor (Fig 8). The planing hull with 20 deg deadrise angle reduces resistance in the range of 19-25% (Table 7) and trim in the range of 53-60% (Table 8) for the hull with interceptor-flap at beam Froude number of 1.57-2.28. On similar lines, the planing hull with interceptor and trim tab of 10 deg deadrise angle showed reduction in resistance and trim for volume Froude number range of 0.6-1.5 (Mansoori et al., [19]), further the study on deep V ship with interceptor and flap (Song et al., [28]) showed trim and drag reduction for Froude number range of 0.33-0.58 which is below planing speed. It is noted that with increasing speed, there is large reduction in trim in the case of interceptor-flap combination in the present study where planing speeds are considered.

Table 7: Percentage reduction in resistance with interceptor, interceptor-4deg flap combination in comparison with bare hull for different speeds

Fn	R_t (%reduction) Interceptor	R_t(%reduction) Interceptor-flap
1.57	25.32	24.45
1.78	22.68	24.78
2.0	20.57	23.45
2.28	20.32	19.52

Table 8**:** Percentage reduction in trim with interceptor, interceptor-4deg flap combination in comparison with bare hull for different speeds

Fn	Trim (%reduction) Interceptor	Trim (%reduction) Interceptor-flap
1.57	33.63	53.03
1.78	38.38	57.35
2.0	41.26	58.73
2.28	44.82	60.51

At the design speed there is acceptable advantage in percentage reduction of resistance and running trim with interceptor and flap combination. Fig 9 shows the percentage reduction of resistance and trim for the vessel fitted with interceptor and interceptor-flap with 4deg. When interceptor is integrated with flap of 4deg angular orientation it is perceived that there is good decrease in trim as well as resistance. At the design speed there is up to 19% of reduction in vessel trim and 2% in drag with interceptor-4deg flap when compared with interceptor.

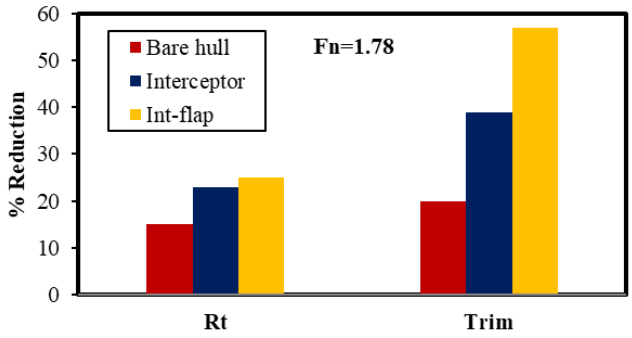

Figure 9: Comparison of percentage reduction in resistance and trim at Fn=1.78 for interceptor and interceptor-4deg flap with bare hull as base case.

4.2 THE FREE SURFACE WAVE PATTERN IN CALM WATER

In calm waters, the Kelvin wave pattern is seen when the vessel moves. The Froude number has a significant influence on this wave pattern (Fig 10). Previous studies also found that in transition mode most of the energy is transferred from hull to water. This energy loss is decreased in the displacement and planing mode. It is common phenomena, a certain amount of energy is transferred from the hull to water but when interceptor is fitted the fuel consumption is reduced due to reduction of vessel resistance and free surface wave elevation reduces wave resistance.

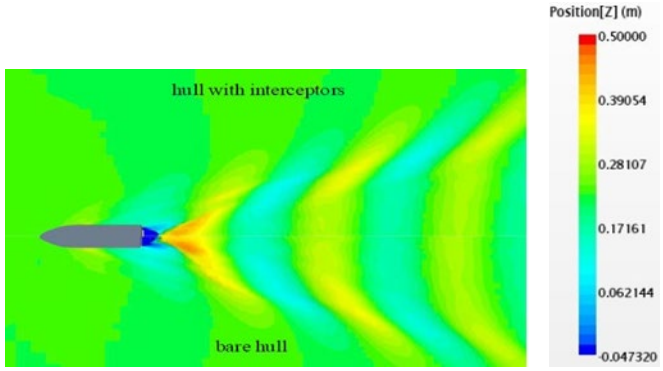

(a) Transition mode

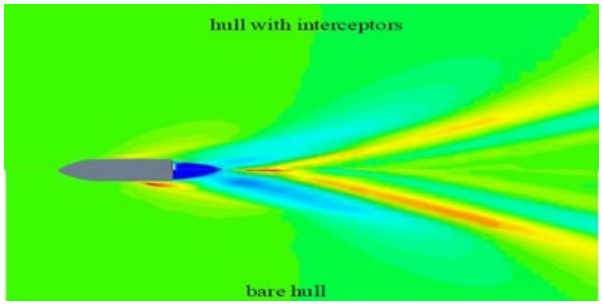

(b) Planing mode

Figure 10: Comparison of free surface wave pattern for transition and planing modes in calm water for bare hull and interceptor at design speed.

With increase in speed, significant hydrodynamic forces are induced causing drastic change in trim and wetted surface of the vessel. Rather than wetting the transom, flow easily separates from the edges. It is also seen that a rooster tail forms behind the stern and accelerates its movement downstream. The wave pattern changes in such a way that it becomes narrow with increasing speed. The trough of stern waves is reduced when interceptor is fitted. Also further reduction in stern wave is observed when interceptor-flap combination is used.

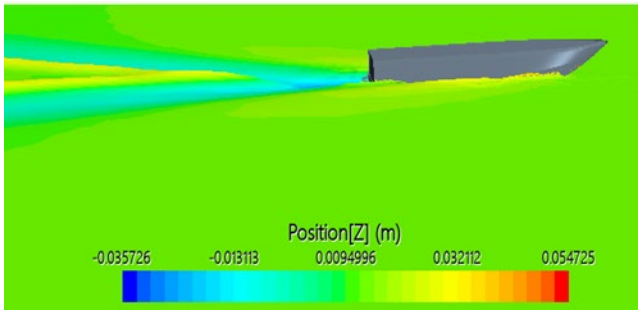

Figure 11: Free surface height near transom at Fn=1.78 for hull with interceptor-4deg flap

Free surface height for the hull with interceptor-4deg flap at Fn =1.78 is illustrated in Fig 11. From contour plot scale, it is perceived that the height of free surface is decreased at the stern when the hull is fitted with interceptor-4deg flap. The vessel is raised upward at the stem indicating that the trim of the vessel is high without appendage device as discussed in Suneela et al., [29,30]. The trim of the hull mounted with interceptor-4deg flap at Fn=1.78 is 2.9 degrees whereas for the bare hull the trim is 6.6 deg and for the hull fitted with interceptor the trim is 4.5deg. The reduction in wave elevation at the transom on free surface shows reduction in wave resistance on the hull.

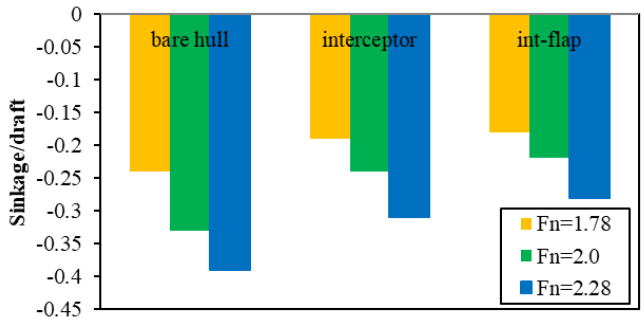

Figure 12: Non-dimensionalised sinkage for the hull, interceptor and integrated interceptor flap for different Froude numbers.

When a vessel advances through water it undergoes sinkage and trim due to variation of hydrodynamic pressure distribution in the longitudinal direction. The sinkage of the hull increases with speed. The wetted surface area marginally increases from bare hull to hull with interceptor and then to hull with interceptor+flap. Smaller contribution in this area is contributed by the interceptor and flap, whereas the major contribution is due to the trim reduction. Fig 12 displays the sinkage for different Froude numbers is given for different configurations (bare hull, interceptor and interceptor-flap). It is perceived that the sinkage is decreasing when hull is fixed with interceptor and interceptor-flap which helps in resistance reduction and further with less fuel consumption.

4.3 WAVE ELEVATION AT THE FREE SURFACE NEAR TRANSOM

The numerical simulations performed in this study captures wave elevation at the free surface for different speeds in calm water for the hull mounted with and without interceptor and interceptor-4deg flap. The wave elevation of the hull for the three cases is captured and observed to have a reduction for the hull with interceptor and further reduction in the case of interceptor and flap combination at different speeds.

The wave elevation for the vessel with and without interceptor -4deg flap near the transom are compared for Fn =1.57-2.28 as shown in Fig 13. With the increase in speed, the stern wave elevation is decreased in calm water case.

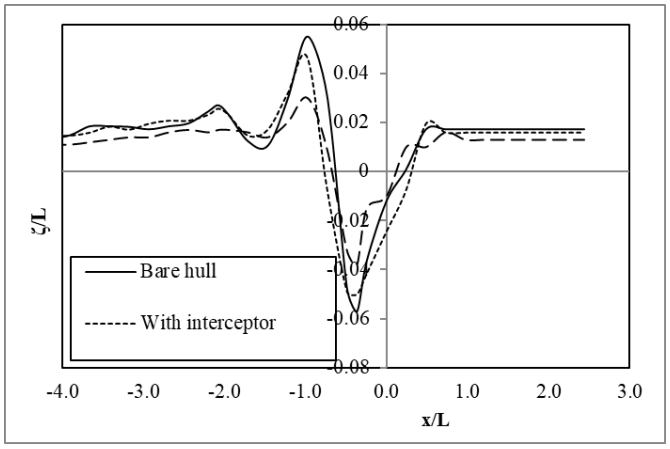

(a) Fn=1.57

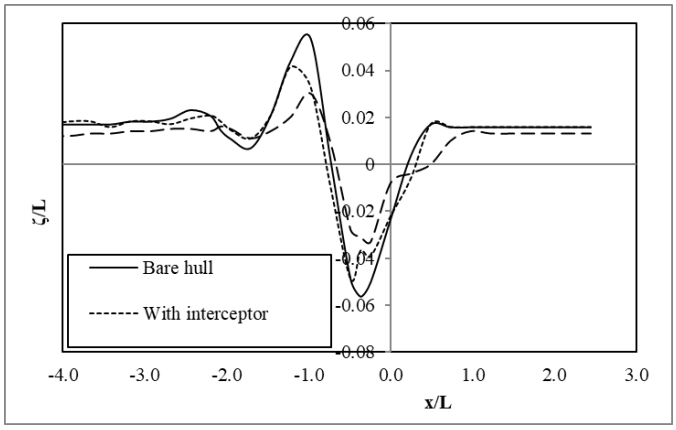

(b) Fn=1.78

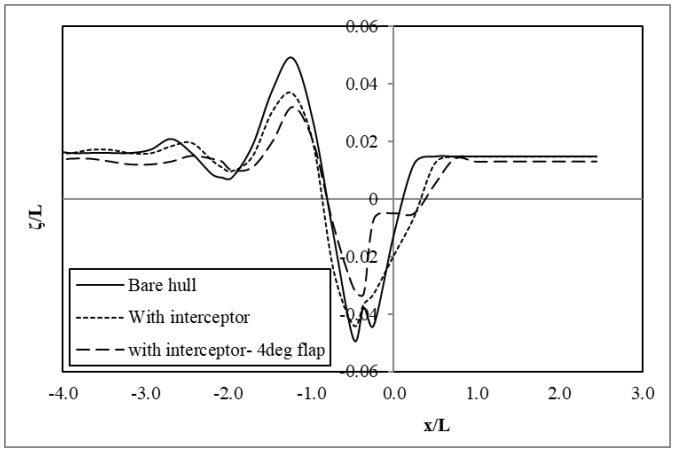

(c) Fn=2.0

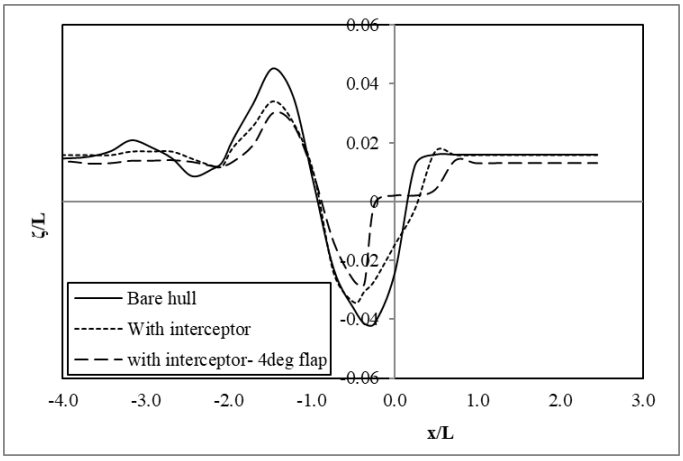

(d) Fn=2.28

Figure 13: Comparison of wave elevation for the bare hull and hull with interceptor and interceptor-4 deg flap for different speeds.

The wave elevation is reduced by 40% at design speed of Fn=1.78 for hull with interceptor-4deg flap when compared to the hull without interceptor-4deg flap. The literature related to integrated interceptor-flap combination and the free surface elevation for planing hulls is very meagre. The reduction in wave elevation at the transom is 25-40% for the hull with interceptor-4deg flap for different speeds. It is observed that the stern wave behind transom is moving further downstream with an increasing speed when fitted with integrated interceptor-flap. The decrease in stern wave helps in reduction of wave resistance accounting in the further reduction of total resistance of the vessel. The reduction in total resistance supports in the economy of fuel consumption.

Table 9: Comparison of wave elevation and percentage reduction near transom with and without interceptor at Fn=1.78

x/L	ζ/L(bare hull)	ζ/L(interceptor)	% reduction
0	-0.0232	-0.02198	5.25
-1	0.053724	0.041	22.72
-1.5	0.020757	0.015	29.41
-2.5	0.023199	0.018	21.05

Table 10: Comparison of wave elevation and percentage reduction near transom with and without interceptor-flap at Fn=1.78

x/L	ζ/L(bare hull)	ζ/L(interceptor-flap)	% reduction
0	-0.0232	-0.008	65.51
-1	0.053724	0.02	62.77
-1.5	0.020757	0.015	27.73
-2.5	0.023199	0.013	43.96

The reduced wave elevation near transom for the hull mounted with interceptor and interceptor-flap is compared with bare hull at Fn=1.78 is shown in Table 9 and 10. Reduction in wave elevation is observed near transom at different points and perceived that the integrated interceptor-flap has more reduction. The reduction in wave elevation helps in the decrease of wave resistance which further supports in the total resistance reduction.

5. SUMMARY AND CONCLUSION

Planing hull model is considered for the study of wave elevation at the transom with and without interceptor and integrated interceptor-flap. The resistance and trim of the craft are studied numerically and are verified and validated with experimental results. The numerical study using RANSE solver was found to give good correspondence with experimental results. So, the numerical study is further extended and discussed on the free surface wave pattern and wave elevation for the hull with and without interceptor-flap in calm water.

The conclusions drawn from the study are

- For various Froude number, a decrease in resistance and trim is noted for the hull equipped with an interceptor-4-degree flap in comparison to the bare hull.
- When the hull with the interceptor-4 deg flap accelerates, the wave elevation decreases. This stern wave's lower elevation contributes to the vessel's decreased wave resistance.
- The vessel's overall resistance reduction of about 19-24% and trim of 50-53% is observed on the vessel.
- Compared to the bare hull in calm water, the stern wave elevation is reduced by 40% at design speed of 25 knots for the hull with interceptor-4deg flap.
- In calm water, the investigation on the hull with the interceptor-4 degree flap for varying speeds revealed a 25–40% reduction in wave elevation close to the transom.

6. ACKNOWLEDGEMENTS

Authors acknowledge the support of IIT Madras through Half-Time Research Assistantship during my PhD in the Department of Ocean Engineering.

7. DECLARATIONS

No competing interests of financial or personal nature.

8. AUTHOR CONTRIBUTION

Conceptualization, Data curation, Methodology, Investigation, Writing – original draft, Investigation, Validation, Formal analysis, Writing – original draft.

9. DATA AVAILABILITY

The datasets used and/or analysed during the current study available from the corresponding author on reasonable request.

10. FUNDING

The author(s) received no financial support for the research, authorship, and/or publication of this article.

REFERENCES

1. ALESSANDRINI, B., and DELHOMMEAU, G (1994). "Simulation of three-dimensional unsteady viscous free surface flow around a ship model*." International Journal for Numerical Methods in Fluids* 19.4: 321-342.
2. SAADIA, A., OMAR, I., AOUNALLAH, M., BELKADI, M., (2015). Numerical Simulation of Free Surface Water Wave for the Flow around NACA 0012 Hydrofoil and Wigley Hull Using VOF Method. World Academy of Science, Engineering and Technology International Journal of Mechanical and Mechatronics Engineering Vol:9, No:5.
3. AHMED, Y M, (2011). Numerical simulation for the free surface flow around a complex ship hull form at different Froude numbers, *Alexandria Engineering Journal*, 50, 229-235.
4. BRIZZOLARA, S., (2003). "Hydrodynamic Analysis of Interceptors with CFD methods" *Proc. Seventh International Conference on Fast Sea Transportation* (FAST), Vol. 3.
5. BRIZZOLARA, S., and SERRA, F. (2007). Accuracy of CFD Codes in the Prediction of Planing Surfaces Hydrodynamic Characteristics. *2nd International Conference on Marine Research and Transportation*. Ischia.
6. CD-ADAPCO, (2014). STAR CCM, User's guide version 9.06.
7. DAWSON, C W., (1977). A practical computer method for solving ship wave problems, *Proceedings of the 2nd International Conference on Numerical Ship Hydrodynamics*, Berkeley, CA, pp. 30–38.
8. DE LUCA, F., MANCINI, S., MIRANDA, S., and PENSA C, (2016). An extended verification and validation study of CFD simulations for planing hulls, *Journal of Ship Research* 60 (2) 101–118.
9. GHASSEMI, H., MANSOURI, M., and ZAFERANLOUEI, S., (2011). Interceptor hydrodynamic analysis for handling trim control problems in the high speed crafts. *Proc. IMechE* Vol 225, 2597-2618. https://doi.org/10.1177/0954406211406650. Part C: *J. Mech Engineering Science*.
10. GHASEMI, H, IRANMANESH, M, ARDESHIR, A., (2010). Simulation of free surface wave pattern due to the moving bodies.
11. HIRT C W., and NICHOLS, B D., (1981). Volume of fluid (VOF) method for the dynamics of free boundaries, *Journal of computational physics*. 39 (1) 210-225.
12. HINO, T., (1987). "Numerical simulation of a viscous flow with a free surface around a ship model." 日本造船学会論文集 1987.161: 1-9.
13. ITTC, (2011). Recommended Procedures and Guidelines Practical Guidelines for Ship CFD Applications 7.5-03-02-03.
14. IN KIM., RYONG PARK-I., KWANG-SOO KIM., and SUAK-HO VAN., (2005). Numerical Simulation of Turbulent Free-Surface Flow around a Self-Propelled Ship, *Proceedings of the Fifteenth International Offshore and Polar Engineering Conference*, Seoul, Korea, June.
15. JENSEN, G.,and SODING, H. (1986). Rankine methods for the solution of the steady wave resistance problem, in *Proceedings of the 16th Symposium on Naval Hydrodynamics*, pp. 575–582.
16. REZA, J M., BINNS, J R., RENILSON, M R., and THOMAS, G., (2012). The prediction of wave patterns at large distances from a moving body in a confined channel. *18th Australasian Fluid Mechanics conference*, Australia, 3-7 December.
17. LARSSON, L., BROBERG, L., KIM, K.J., ZHANG, D H., (1989). New viscous and inviscid CFD techniques for ship flow, in *Fifth International Conference on Numerical Ship Hydrodynamics,* Hiroshima, Japan, pp. 1–25.
18. MARONNIER, V., PICASSO, M, RAPPAZ, J., (1999). Numerical simulation of free surface flows, Journal of Computational Physics 155, 439–455.
19. MANSOORI, M., FERNANDES, A C., GHASSEMI H., (2017). Interceptor design for optimum trim control and minimum resistance of planing boats. Journal of *Applied Ocean Research*. https://doi.org/10.1016/j.apor. 10.006.
20. PRASAD, B., HINO, T., SUZUKI, K., (2015). Numerical simulation of free surface flows around shallowly submerged hydrofoil by openfoam, *Ocean Engineering* 102, 87,94.
21. QIUXIN, G., (2002). "Numerical simulation of free surface flow around ship hull. "*Journal of Ship Mechanics* 6.3: 1-13.
22. STERN, F., WILSON, R., COLEMAN, H., and PATERSON, E. **(**2001). 'Comprehensive approach to verification and validation of CFD simulation Part 1: Methodology and Procedures', *Journal of Fluids Engineering*, 123, no. 4, December, pp. 793-802.
23. SADATHOSSEINI, S H., MOUSAVIRAAD, S M., FIROOZABADI, B., and AHMADI, G. (2006). Numerical Simulation of Free-Surface Waves and Wave Induced Separation, *Scientia Iranica*, Vol. 15, No. 3, pp 323-331.
24. SALAS, M., GONZALO, T., (2013). Assessment of Appendage effect on forwarding resistance reduction,

Ship Science and Technology, Vol 7-n. 13-(37-45), Cartagena (Columbia).

26. SEO, K., GOPAKUMAR, W., MEHMET, A., (2013). Experimental investigation of dynamic trim control devices in fast speed vessel, *Journal of Navig. Port Res.* Vol. 37, No. 2: 137-142.
26. JANGAM, S., KRISHNANKUTTY, P, ANANTHA SUBRAMANIAN, V., (2018). Numerical study on the hydrodynamic performance of integrated interceptor-flap fitted to the transom of planing hull, *Proceedings of the ASME, 37th International conference on Ocean, Offshore and Arctic Engineering*, OMAE, Madrid, June.
27. SONG, K, GUO, C, WANG, C, GONG, J, LI, P, (2018*a*). Investigation of the influence of an interceptor on the inlet velocity distribution of a waterjet-propelled ship using SPIV technology and RANS simulation. *Journal of Ships and Offshore Structures*. Pp 138-152.
28. SONG, K, GUO, C, WANG, C, GONG, J, LI, P, (2018*b*). Influence of interceptors, stern flaps and their combination on the hydrodynamic performance of deep V ship. *Journal of Ocean Engineering*, 170:306-320.
29. JANGAM, S., KRISHNANKUTTY, P, ANANTHA SUBRAMANIAN, V., (2020). Numerical investigation on the hydrodynamic performance of high-speed planing hull with transom interceptor. *Journal of Ships and Offshore Structures*. DOI: 10.1080/17445302.2020.1738134.
30. JANGAM, S., KRISHNANKUTTY.P, ANANTHA SUBRAMANIAN, V., (2021). Hydrodynamic performance of planing hull with interceptor-flap hybrid combination. Journal of Ocean Engineering and Marine Energy.
31. TUCK, E O., SCULLEN, D C., and LAZAUSKAS, L., (2002). Wave Patterns and Minimum Wave Resistance for High-Speed Vessels. *24th Symposium on Naval Hydrodynamics*, Fukuoka, JAPAN, 8-13 July.
32. TEZDOGAN, T, DEMIREL, Y K., KELLET, P., KHORASANCHI, M., INCECIK, A., (2015). Full-Scale unsteady RANS-CFD simulations of ship behaviour and performance in head seas due to slow steaming, *J. Ocean Eng*. 97 186–206.
33. VILLA, D., and BRIZZOLARA, S., (2009). A systematic CFD analysis of flaps /interceptors hydrodynamic performance, *Proceedings of 10th International Conference of Fast Sea Transportation*, Athens, Greece.
34. XIA, F., (1986). Calculation of lifting flow with free surface, SSPA Report no. 2912-2 (SSPA Maritime Research and Consulting, Sweden, 1-62.
35. ZHANG, ZHI-RONG, FENG ZHAO, and BAIQI LI. (2002). "Numerical calculation of viscous free-surface flow about ship hull." *Journal of ship mechanics* 6.6: 10-17.